Published in final edited form as:
Int J Cancer. 2014 January 1; 134(1): 9–20. doi:10.1002/ijc.28327.

Alternatively spliced tissue factor contributes to tumor spread and activation of coagulation in pancreatic ductal adenocarcinoma

Dusten Unruh[1,*], **Kevin Turner**[2,*], **Ramprasad Srinivasan**[1,*], **Begüm Kocatürk**[3], **Xiaoyang Qi**[1], **Zhengtao Chu**[1], **Bruce J. Aronow**[4], **David R. Plas**[5], **Catherine A. Gallo**[5], **Holger Kalthoff**[6], **Daniel Kirchhofer**[7], **Wolfram Ruf**[8], **Syed A. Ahmad**[9], **Fred V. Lucas**[2], **Henri H. Versteeg**[3,*], and **Vladimir Y. Bogdanov**[1,*]

[1]Division of Hematology/Oncology, Internal Medicine, University of Cincinnati College of Medicine, Cincinnati, OH [2]Department of Pathology & Laboratory Medicine, University of Cincinnati College of Medicine, Cincinnati, OH [3]Einthoven Laboratory for Experimental Vascular Medicine, Leiden University Medical Center, Leiden, The Netherlands [4]Department of Biomedical Informatics and Developmental Biology, Cincinnati Children's Hospital and Medical Center, Cincinnati, OH [5]Department of Cancer Biology, University of Cincinnati College of Medicine, Cincinnati, OH [6]University Hospital Schleswig-Holstein, Institute of Experimental Cancer Research, Kiel, Germany [7]Department of Early Discovery Biochemistry, Genentech, Inc., San Francisco, CA [8]Department of Immunology and Microbial Science, The Scripps Research Institute, La Jolla, CA [9]Department of Surgery, University of Cincinnati College of Medicine, Cincinnati, OH

Abstract

Alternatively spliced tissue factor (asTF) promotes neovascularization and monocyte recruitment *via* integrin ligation. While asTF mRNA has been detected in some pancreatic ductal adenocarcinoma (PDAC) cell lines and increased asTF expression can promote PDAC growth in a subcutaneous model, the expression of asTF protein in bona fide PDAC lesions and/or its role in metastatic spread are yet to be ascertained. We here report that asTF protein is abundant in lesional and stromal compartments of the five studied types of carcinoma including PDAC. Analysis of 29 specimens of PDAC revealed detectable asTF in >90% of the lesions with a range of staining intensities. asTF levels in PDAC lesions positively correlated with the degree of monocyte infiltration. In an orthotopic model, asTF-overexpressing high-grade PDAC cell line Pt45P1/asTF+ produced metastases to distal lymph nodes, which stained positive for asTF. PDAC cells stimulated with and/or overexpressing asTF exhibited upregulation of genes implicated in PDAC progression and metastatic spread. Pt45P1/asTF+ cells displayed higher coagulant activity compared to Pt45P1 cells; the same effect was observed for cell-derived microparticles (MPs). Our findings demonstrate that asTF is expressed in PDAC and lymph node metastases and

Correspondence to: Vladimir Y. Bogdanov, Division of Hematology/Oncology, University of Cincinnati College of Medicine, 3125 Eden Avenue, Cincinnati, OH 45267, USA, Tel: +001-513-558-6276, Fax: +001-513-558-6703, vladimir.bogdanov@uc.edu.
*D.U., K.T., R.S., H.H.V. and V.Y.B. contributed equally to this work

potentiates PDAC spread *in vivo*. asTF elicits global changes in gene expression likely involved in tumor progression and metastatic dissemination, and it also enhances the pro-coagulant potential of PDAC cells and cell-derived MPs. Thus, asTF may comprise a novel therapeutic target to treat PDAC and, possibly, its thrombotic complications.

Keywords

pancreatic ductal adenocarcinoma; metastasis; molecular mechanisms of angiogenesis; tissue factor; alternative splicing Additional supporting material for online publication has been included

---

Pancreatic cancer is the fourth leading cause of cancer-associated death, and pancreatic ductal adenocarcinoma (PDAC) accounts for 85% of all forms of pancreatic cancer.[1] Several forms of solid malignancies are associated with a hypercoagulant state, which is thought to be partially caused by increased tissue factor (TF) expression on tumor cells due to, *e.g.*, activation of proto-oncogenes such as *K-ras*, *EGFR* as well as inactivation of tumor suppressor genes such as *p53* and *PTEN*.[2] TF-bearing MPs have also been thought to play a critical role in malignancy-associated venous thromboembolism (VTE). Indeed, several studies indicate that cancer patients with VTE have significantly higher TF-MP activity and levels than cancer patients without VTE,[3,4] and such a link between TF-MP and VTE is confirmed by mechanistic studies.[5] Alternatively spliced TF (asTF) is a minimally coagulant isoform of full-length tissue factor (flTF) that drives angiogenesis nonproteolytically through binding to integrins α6β1 and αvβ3.[6,7] asTF-integrin interaction results in the activation of key signaling intermediates such as PI3K/Akt, p38 MAPK and FAK, resulting in endothelial neovascularisation.[7] Moreover, asTF binding to β1 integrins on microvascular endothelial cells activates the NF-kB pathway that results in the increased expression of major cell adhesion molecules such as E-selectin, VCAM-1 and ICAM-1, leading to enhanced monocyte adhesion to, and migration through, endothelial cells.[8] Of note, α6β1 is expressed on PDAC cells, and the levels of this integrin are greatly potentiated by IL-1α; moreover, α6β1 induces Ras/ERK signaling resulting in the increased proliferation and migration of PDAC cells.[9] To date, studies of asTF in the cancer setting have been focused largely on cervical[7,8] and lung cancer: in 2008, asTF mRNA was found to be increased in squamous cell carcinoma of the lung, as well as pulmonary adenocarcinoma.[10] In tissues of non-small cell lung cancer, asTF mRNA levels are highly predictive of patient outcome.[11] Studies of asTF in the PDAC setting have thus far been limited. In 2006, screening of eight low- and high-grade PDAC-derived cell lines detected asTF mRNA expression in six cell lines.[12] In 2007, Hobbs *et al*. reported that overexpression of asTF in a TF-null PDAC line MiaPaCa-2 enhances tumor growth in a subcutaneous model; however, this study suffered from lack of mechanistic insight as well as conceptual limitations inasmuch as asTF was studied in a nonphysiologic, flTF-null setting.[13] While the expression of flTF is well documented in human PDAC (Ref. [14] and work cited therein), it is yet to be established whether asTF mRNA and/or protein are expressed in bona fide human pancreatic cancer tissue. No data are available regarding the functional contribution(s) of asTF to PDAC pathobiology in a physiologically relevant *in vivo* setting.

In this study, we report for the first time that asTF (*i*) is expressed in human PDAC tumor tissue exhibiting heavy monocyte infiltration, (*ii*) promotes tumor metastasis in an orthotopic model of PDAC, (*iii*) exerts autocrine effects on PDAC cells resulting in global changes in gene expression and (*iv*) contributes to the procoagulant potential of PDAC cells and cell-derived MPs *via* distinct mechanisms.

Material and Methods

Reagents

Human anti-asTF rabbit polyclonal antibody suitable for immunohistochemical studies was described and characterized previously.[8,15] Custom rabbit monoclonal antibodies RabMab1 (asTF-specific) and RabMab95 (recognizing a TF region shared by asTF and flTF) were employed in Western blotting and ELISA assays. For on-cell Western assays and flow cytometry analysis of intact cells and cell-derived MPs, flTF-specific mouse monoclonal antibody 10H10[8] and the rabbit monoclonal antibody RabMab1 were used. Anti-GAPDH rabbit polyclonal antibody was from Trevigen, Inc. Isolectin B4 was from Invitrogen (Carlsbad, CA). Anti-integrin β1/β3 and EGFR antibodies were from R&D Systems (Minneapolis, MN) and Biolegend (San Diego, CA), respectively. TaqMan probe/-primer sets for EFEMP1, AREG and VEGFA were from Roche Applied Science (Indianapolis, IN). Anti-EFEMP1 polyclonal antibody was from Thermo Scientific (West Palm Beach, FL). Anti-total MAPK/p-MAPK and total Akt/p-Akt antibodies were from Cell Signaling Technology (Beverly, MA). Anti-CD68 antibody was from Imgenex (San Diego, CA). Anti-F4/80 antibody was from Biolegend. Mouse monoclonal anti-human TF antibody 7G11[16] was used as an inhibitory antibody in TF activity assays.

Tumor tissue specimens

Commercial tissue microarrays (TMA) were purchased form Imgenex Corporation (San Diego, CA). Use of de-identified specimens of human PDAC tissue was approved by the Institutional Review Board, University of Cincinnati. Twenty-nine specimens of primary PDAC tissue harvested from 26 patients were examined; in addition, five specimens of seminal lymph node metastases from four patients were available for and subjected to histological analysis. The summary of clinicopathological characteristics of the PDAC cohort is provided in Supplementary Table 1, Supporting Information. Immunohistochemical and fluorescence studies were performed as previously described[8]; asTF staining intensity was annotated by two trained anatomical pathologists based on the strength of the reaction obtained by HRP color substrate DAB. PDAC specimens were stratified into the weak, moderate and strong subcohorts based on the staining intensity of ≥75% of tumor cells whose staining pattern was predominantly intracellular in nature; extracellular/stromal staining, when present, was also considered in scoring.

Cell lines

Pt45P1 is a grade III human PDAC cell line that features key mutations characteristic of PDAC and has been previously shown to produce grade III tumors in nude mice.[17] Capan-1, a grade I human PDAC cell line, was obtained from ATCC (Manassas, VA). Cells were

cultured in IMDM (Capan-1) and DMEM (Pt45P1) supplemented with FBS in the presence of antibiotics/antimycotics and selective antibiotics, when appropriate.

Overexpression of asTF in Pt45P1 cells

asTF open reading frame was subcloned in pSecTagA (Invitrogen, Carlsbad, CA) using restriction sites NheI and AgeI, and the integrity of the resultant expression construct was verified using automated sequencing. The linearized construct was transfected into Pt45P1 cells using Fugene HD (Roche, Indianapolis, IN), and asTF-overexpressing clones were obtained using escalating concentrations of Zeocin as per the manufacturer's instructions, were pooled and expanded to establish asTF-overexpressing line Pt45P1/asTF+.

Western blotting

Cells were grown to confluence in six-well plates, washed twice with PBS, lysed using 2X sample buffer containing 2-mercaptoethanol and denatured at 95°C for 5 min. The lysates were loaded on 10% polyacrylamide gels and transferred to PVDF membrane. The membrane was blocked for 1 hr using 5% nonfat milk and probed with the appropriate primary and the corresponding HRP-conjugated secondary antibodies (Invitrogen) using conventional techniques. The blots were developed using LumiLight (Roche), and chemiluminescent bands were visualized by exposure to X-ray film. To verify equal loading, blots were then stripped and re-probed for GAPDH.

Flow cytometry, ELISA and on-cell western assays

Levels of various proteins and phosphatidylserine (PS) on the surface of nonpermeabilized cells and/or cell-derived MPs was measured using flow cytometry; in brief, PDAC cells and cell-derived MPs were suspended in 50 μL of PBS or Annexin V staining buffer (Invitrogen), to which 10 μg of the corresponding primary antibodies or 10 μL of Annexin V-FITC (Invitrogen) were added and incubated at RT for 30 min. The cells were then washed twice with PBS, resuspended in 500 μL of PBS, incubated with the corresponding secondary antibodies (excluding Annexin V-FITC samples), washed twice with PBS and analyzed; isotype IgG whole molecule preparations (Jackson Immunoresearch) served as negative/background controls. All flow cytometry studies were performed using FACS Calibur (Becton Dickinson). Levels of asTF in the conditioned medium were assessed using a sandwich ELISA; in brief, sample aliquots were placed in 96-well plates pre-coated with the capture antibody RabMab95 and incubated for 2 hrs; after subsequent washes, HRP-conjugated detection antibody RabMab1 was added for 1 hr, unbound antibody washed away, o-Phenylenediamine was added and the plate was read at 405 nm in a colorimetric assay using a VersaMax microplate reader (Molecular Devices, Sunnyvale, CA). For on-cell Western assays, intact cells (2×10^4 cells per well, Pt45P1 and Pt45P1/asTF+) were seeded in 96-well plates, washed free of media with PBS and flash-fixed in 4% paraformaldehyde for 5 min at room temperature. Cell surfaces were then blocked with 1X Power-Block (Biogenex, CA) and probed with the monoclonal flTF-specific antibody 10H10 and secondary anti-mouse IR-dye-800 CW (LI-COR Biosciences, Lincoln, NE) to assess cell-surface flTF expression; imaging was carried out using Odyssey IR scanner and quantified using Odyssey software (both from LI-COR).

Microarray analysis

Pt45P1 and Capan-1 cells were treated with recombinant human asTF preparations generated and characterized as previously described[7] for 4 hrs at a final concentration of 50 nM; equal volumes of 50% glycerol in PBS served as the vehicle control. Total RNA was isolated using RNAeasy Kit (Qiagen, Valencia, CA), reverse transcribed, amplified, fragmented and labeled for microarray analysis using the Nugen WTA Ovation FFPE kit and Encore biotin module (Nugen, San Carlos, CA) according to the manufacturer's instructions. The labeled samples were hybridized onto Affymetrix Human Gene 1.0 ST chips. Transcripts that were differentially expressed in Capan-1 and Pt45P1 cells—untreated and/or as a result of asTF treatment—were identified based on filtering for probe sets with Robust Multichip Average-normalized raw expression of at least 1.5-fold with $p < 0.05$ using a Welch t-test; the results of the analysis were uploaded to NCBI GEO (http://www.ncbi.nlm.nih.gov/geo/query/acc.cgi?acc=GSE45928). Differences in gene expression between Pt45P1 and Pt45P1/asTF+ cells were assessed using RNAseq technology. Samples from each cell line were analyzed in duplicate using Illumina TruSeq mRNA cDNA libraries that were sequenced using single-end 50 base reads at a depth of ~20 million reads on an Illumina 2500 analyzer; the results were uploaded to NCBI (http://www.ncbi.nlm.nih.gov/sra?term=%28SRP020496%29). Gene list enrichment analysis was performed using ToppGene (http://toppgene.cchmc.org/).

Isolation of cell-derived MPs

5×10^5 Pt45P1 and Pt45P1/asTF+ cells were seeded in a T-75 flask and grown to confluence over 2 days. The cells were then switched to serum-free defined media for 4 days, after which the conditioned media was collected and pre-centrifuged at 5,200*g* for 1 hr to remove cell debris. The resultant MP-containing supernatant was ultra-centrifuged at 337,000*g* (NVTi 65.2 rotor, Beckman) for 2.5 hrs. The supernatant was carefully aspirated using a vacuum manifold and the remaining MP pellet was resuspended in PBS and used in flow cytometry analyses and/or Factor Xa generation assays.

Two-step FXa generation assay

5×10^3 intact cells or 70 μL of cell-derived MP resuspended in HBS were incubated with FVIIa (Enzyme Research Laboratories, South Bend, IN) at the final concentration of 10 nM for 15 min to pre-form a TF.VIIa complex. Subsequently, FX (Enzyme Research Laboratories) was added to the samples at the final concentration of 100 nM and allowed to incubate for another 15 min, after which $CaCl_2$ was added to initiate FXa generation. The reaction was stopped at 15 min using EDTA-Bicine, and FXa substrate Pefachrome (Enzyme Research) was then added and OD 405 nm recorded over a period of 1 hr using VersaMax microplate reader (Molecular Devices). All reactions were performed at 37°C.

In vivo studies

Use of laboratory animals and the experimental protocols were approved by the Institutional Animal Care and Utilization Committee, University of Cincinnati. PDAC cells (1×10^6 in 150 μL PBS) were orthotopically implanted in the pancreases of nude mice (age: 8 weeks; source: Harlan Laboratories, Indianapolis, IN; $n = 3$ per cohort, three independent

experiments); 3 weeks post-surgery, *in vivo* imaging was performed using *in vivo* multispectral imaging system FX (Kodak) employing a novel method to target tumors by Cell-Vue Maroon (CVM)-labeled, nanovesicle-coupled Saponin C protein fragment H2 (CVM-SapC[H2]-DOPS): such nanovesicles selectively target tumor cells as well as tumor vasculature enriched in externalized phosphatidylserine.[18] For quantification of tumor spread to distal lymph nodes, the images were analyzed in the corresponding anatomical locations or projections above and below the limbs in the lateral view using Carestream MI software, background fluorescence subtracted, data converted to photons per second per mm^2, and the results averaged. Following imaging studies, animals were sacrificed by intracardiac puncture, tissue specimens were harvested, fixed in formalin, embedded in paraffin and 4-μm sections analyzed using conventional techniques.

Statistical analysis

Student's *t*-test was used to assess the statistical significance of the differences between the groups; $p < 0.05$ was considered significant. For multiple group comparisons, one-way ANOVA was used and Tukey post-hoc test was applied to derive *p* values.

Results

asTF protein levels in human PDAC tissue positively correlate with the density of stromal monocytic infiltrates

To assess whether asTF protein is detectable in several forms of solid malignancies including PDAC, we performed IHC staining for asTF in commercial microarrays (TMA) comprising PDAC ($n = 10$), breast ($n = 10$), urothelial ($n = 10$), prostate ($n = 9$) and ovarian ($n = 10$) carcinoma. asTF immunoreactivity was observed in all examined tumor tissues, including pancreatic intraepithelial neoplasia (PanIN)—early-stage PDAC lesions—as well as advanced PDAC (Fig. 1*a*). We also co-stained these tumor sections for CD68, a monocyte/macrophage marker, and observed strong asTF expression in tumor-infiltrating monocytes; nearly all tumor-infiltrating monocytes expressed asTF, demonstrating that stroma cells, in addition to tumor cells, can also serve as a source of asTF in malignant tissue (Fig 1*b*). Among the solid tumors studied, PDAC had the most monocyte infiltration, approximately twofold over the other four solid malignancies ($p < 0.05$, Fig 1*c*); of note, eight out of 10 PDAC specimens had some degree of detectable monocytic infiltration, whereas in the other four groups of specimens, monocyte infiltration was observed in ≤4 out of ten per group. We then examined 29 specimens of resected PDAC tissue for asTF expression. There was no appreciable staining for asTF in the normal pancreatic tissue (areas adjacent to the tumor lesions, available in ~30% of all PDAC specimens examined) with the exception of islets of Langerhans exhibiting consistently weak staining; asTF expression was detectable in over 90% of PDAC specimens (Figs. 2*a* and 2*b*). The tumor lesion as well as the associated stroma stained positive for asTF. Occasionally, (peri)nuclear staining pattern was observed for asTF in some PDAC cells (Fig. 2*b*). In regional lymph node metastases, moderate levels of asTF expression were observed. Based on the staining intensity of asTF in tumor lesions, we stratified the 29 PDAC specimens into three categories (weak = five specimens from five patients, moderate = 19 specimens from 17 patients and strong = five specimens from four patients); CD68 staining of the specimens

revealed significantly higher levels of CD68+ infiltrating monocytes in the "strong-asTF" subcohort compared to the "weak" and "moderate" subcohorts (Fig. 2*c*). Isolectin B4 staining revealed paucity of vascularization in PDAC tissue specimens, which is consistent with the notion that PDAC is a hypovascular adenocarcinoma[19]; still, one of the "strong-asTF" specimens exhibited a high degree of vascularization (Fig. S1*a*, Supporting Information). We note that 100% of "strong-asTF" patients presented with perineural invasion, compared to 60% in the "weak-asTF" subcohort and 65% in the entire PDAC cohort (Supplementary Table 1, Supporting Information).

asTF increases metastatic spread of high-grade PDAC cells *in vivo*

a. Characterization of asTF-overexpressing Pt45P1 cell line—To ascertain the role of asTF in pancreatic tumor growth and metastasis, we used two well-characterized cell lines, namely Capan-1 and Pt45P1 cells which are grade I and grade III PDAC lines, respectively. Semi-quantitative RT-PCR revealed that basal expression of asTF mRNA is higher in Pt45P1 cells compared to Capan-1 cells (Fig. 3*a*); we then proceeded to overexpress asTF in Pt45P1 cells to establish the line we termed Pt45P1/asTF+, and verified asTF overexpression by RT-PCR and western blotting. flTF expression appeared somewhat higher in Capan-1 compared to Pt45P1, and in Pt45P1 compared to Pt45P1/asTF+ (Fig. 3*a*). flTF and asTF mRNA expression was then quantified using real-time PCR with reverse transcription, normalized to GAPDH (Fig. 3*b*). Quantitative real-time PCR revealed no significant difference in flTF mRNA levels between Pt45P1 and Pt45/asTF+ cells, and Western blot analysis of total cell lysates revealed no difference in flTF protein levels among the three cell lines, yet asTF levels were higher in Pt45P1 than in Capan-1 cells with Pt45P1/asTF+ displaying the highest levels of asTF protein (Fig. 3*c*). Annexin V staining revealed no significant difference in the levels of externalized phosphatidylserine among the three lines (Fig. 3*d*).

b. asTF overexpression increases the aggressiveness of PDAC in an orthotopic model—Nude mice were injected with 1×10^6 cells of Capan-1, Pt45P1 and Pt45P1/asTF+ ($n = 3$) orthotopically into pancreases, and tumor growth was monitored periodically using CVM-SapC[H2]-DOPS-based *in vivo* imaging (Fig. 3*e*). After 3.5 weeks of orthotopic xenograft, we observed tumor growth in all three sets of mice; statistically significant evidence of enhanced distal metastases was observed in mice injected with Pt45P1/asTF+ cells compared to the Pt45P1 cohort (Fig. 3*f*). The animals were then euthanized and upon necropsy, it became apparent that in Pt45P1/asTF+ mice, tumor cells spread to distal lymph nodes; of note, there were no differences between the cohorts in terms of tumor volume and/or mass at this early stage (not shown). The excised tumors were then formalin–fixed, and paraffin sections stained for asTF which showed various degrees of asTF expression; the lymph node metastases from the Pt45P1/asTF+ mice were also immunoreactive for asTF (Fig. 3*e*). As we previously showed that asTF promotes angiogenesis,[7] we tested the extent of neovascularization in the primary tumors and determined that Pt45P1/asTF+ tumors had the highest vessel density followed by Pt45P1 and Capan-1 tumors ($p < 0.001$) (Fig. 3*g*). F4/80 staining of tumor specimens revealed progressively higher monocyte infiltration of tumor stroma with the increasing levels of

asTF produced by tumor cells (Fig. 3*h*), which is in agreement with the results obtained using human PDAC specimens (Fig. 2*c*).

asTF induces global changes in gene expression in PDAC cells

Recently, it was reported that β1/β3 integrins—both engaged by asTF[6,7]—synergize with EGFR to upregulate several kinases critical to cancer pathbiology.[20,21] To explore whether short-term exposure to asTF protein can elicit autocrine changes in PDAC cells, we treated Capan-1 and Pt45P1 cells with recombinant asTF (50 nM) or vehicle control for 4 hrs and assessed gene expression using microarrays. Out of the 185 genes differentially expressed in Capan-1 and Pt45P1 cells, 19 were relevant to such processes as EGRF signaling, mesenchymal development and epithelial to mesenchymal transition (EMT) (Fig. 4*a*); western blotting revealed upregulation of MAPK and Akt phosphorylation in response to asTF (Fig. 4*b*), and expression of *EFEMP1*—the gene that promotes PDAC growth[22]—was upregulated in response to asTF in both PDAC cell lines (Fig. 4*c*). To explore the gene expression shifts elicited by sustained overexpression of asTF, we compared transcriptomes of Pt45P1 and Pt45P1/asTF+ cells using RNAseq; the results, summarized in Fig. 4*d*, show that asTF promotes upregulation of cell migration, MAPK signaling, EMT and wound healing processes while downregulating cell adhesion, phosphatase activity, inhibition of MAPK cascade and apoptosis; again, upregulation of MAPK activity in response to heightened asTF levels was observed, and increased phosphorylation of Akt was observed in Pt45P1/asTF+ cells compared to Pt45P1 cells when cultures were maintained in low serum (Fig. 4*e*). Interestingly, Pt45P1/asTF+ cells exhibited increased upregulation of *EFEMP1* as well as *AREG*—recently shown to promote proliferation of PDAC cells[23]—and *VEGFA* (Fig. 4*f*); immunohistochemical evaluation of tissue specimens confirmed upregulation of EFEMP1 protein expression in Pt45P1/asTF+ cells (Fig. 4*g*). Surface levels of β1/β3 integrins and EGFR did not differ in Pt45P1 and Pt45P1/asTF+ cells (Fig. S1*b*, Supporting Information).

asTF contributes to the procoagulant potential of PDAC cell lines

The procoagulant potential of asTF is still poorly defined and not universally recognized. asTF requires interaction with phospholipid surfaces to exert its weak procoagulant activity.[6] We measured the TF-dependent procoagulant activity on PDAC cell surfaces using a standard endpoint two-step FXa generation assay. We observed a significant increase in TF activity in Pt45P1/asTF+ compared to Pt45P1 (Fig. 5*a*). Cell-derived MPs isolated from conditioned media of Pt45P1/asTF+ cells also revealed a ~1.5-fold increase in TF activity compared to Pt45P1-derived MPs (Fig. 5*b*). There was no difference in the total number of MP generated by Pt45P1 and Pt45P1/asTF+ cells (Fig. S1*c*, Supporting Information). To confirm the specificity of our assay, we performed control experiments using monoclonal antibody 7G11, which inhibits the activity by hindering TF/VIIa interaction.[16] To address the possible contribution of altered flTF and/or asTF protein levels to the observed increase in pro-coagulant activity, we measured the surface level expression of flTF and asTF. While there was a trend toward a decrease in surface flTF levels on Pt45P1/asTF+ cells compared to Pt45P1 cells, it did not reach significance neither by FACS nor by on-cell western assay; however, MPs generated by Pt45P1/asTF+ cells carried significantly more flTF compared to Pt45P1 cells (Figs. 5*c* and S1*d*, Supporting

Information). Surprisingly, asTF was also detectable on the surface of Pt45P1 and Pt45P1/asTF+ cells and MPs; moreover, asTF surface expression was significantly increased in Pt45P1/asTF+ cells as well as MPs generated by them (Fig. 5*d*); an approximately fivefold increase in the levels of free-secreted asTF protein was also seen in the MP-free conditioned media from the Pt45P1/asTF+ cells compared to Pt45P1 conditioned media (Fig. 5*d*). There was no difference in the levels of β1/β3 integrins on MPs generated by Pt45P1 and Pt45P1/asTF+ cells (Fig. S1*e*, Supporting Information). By ELISA, plasma of mice bearing Pt45P1/asTF+ tumors contained significantly more asTF compared to that of mice bearing Pt45P1 and/or Capan-1 tumors (Fig. 5*e*). Exogenous addition of recombinant asTF resulted in a dose-dependent increase in TF procoagulant activity in Pt45P1 cells, whereas there was no such increase in TF activity when recombinant asTF was added to Pt45P1-derived MP preparations (Fig. 5*f*).

Discussion

In this report, we show for the first time that asTF protein is expressed in human PDAC lesions; asTF is evidently produced by the tumor cells as well as the infiltrating monocytes. Pancreatic tumors tend to be hypovascular in nature, and pharmacokinetics-related issues are commonly associated with the treatment of PDAC.[19] While the human PDAC specimens in our study appeared largely hypovascular, a limitation of our study is that it involved a relatively small number of PDAC specimens and, especially considering heterogeneity of PDAC tissue, better-powered studies involving (*i*) larger cohorts and (*ii*) in-depth examination of a larger tissue volume of each PDAC specimen are thus highly warranted. Still, we invariably found heavy infiltration of monocytes in the tumor stroma; notably, the degree of monocyte infiltration positively correlated with asTF protein levels in PDAC lesions (Fig. 2*c*). The role of the flTF/asTF synergy in cancer pathobiology is very poorly understood. Inflammatory stromal cells and infiltrating monocytes are crucial mediators of lymph-angiogenesis. Lymphatic invasion of the tumor front and lymphatic metastasis is the major determining factor for PDAC metastasis.[24] We previously showed that asTF could act as an inflammatory mediator, inasmuch as its activation of endothelial cells yields enhanced monocyte adhesion and transmigration under chemokine gradients.[8] It is thus reasonable to propose that asTF expressed in the tumor cells and/or tumor-associated macrophages could play a role in PDAC metastasis.

In all biological settings described to date, flTF and asTF are co-expressed; thus, we assessed the role of asTF in pancreatic tumors in an orthotopic model of PDAC using an flTF-expressing PDAC cell line Pt45P1. We find that asTF promotes tumor spread in this model, and it also drives angiogenesis as revealed by the increase in vascular density. We observed an appreciable increase in macrophage infiltration in the orthotopically grown Pt45P1/asTF+ tumors, suggesting that our orthotopic model is suitable to study monocyte recruitment elicited by asTF in a PDAC setting (Fig. 2*c*). Hobbs *et al*.[13] have shown that asTF induces pancreatic tumor growth and angiogenesis in a sub-cutaneous model, but flTF paradoxically had an inhibitory effect on both, in contrast to findings of others who have convincingly determined that flTF expression is positively associated with tumor growth and angiogenesis.[25,26] In this light, the subcutaneous model employed by Hobbs *et al*.[13] has other serious limitations including, most significantly, a complete lack of recapitulation of

the PDAC microenvironment and/or suitability in assessing metastatic potential. Furthermore, the MiaPaCA-2 cell line that was used by Hobbs *et al*.[13] lacks the TF gene expression; since asTF is not found in the absence of flTF, this model is not suitable for assessment of the role of asTF and/or flTF/asTF synergy in tumor growth and metastasis. We observed an increase in tumor vascularization in pancreatic tumors derived from an asTF-overexpressing PDAC cell line, and it is reasonable to speculate that the underlying mechanisms of neovascularization are engaged by integrin-mediated signaling.[7] Our microarray data highlight the signaling changes elicited by asTF in PDAC cell lines. asTF significantly activated various biological processes that are involved in tumorigenesis such as EGFR pathway and epithelial-mesenchymal signaling. One of the genes activated by asTF is *EFEMP1*, whose product is a ligand for EGFR and competes with EGF for receptor binding; EFEMP1 has been shown to activate MAPK and Akt in inducing pancreatic tumor growth.[22,27] Although PDAC tumors tend to be hypovascular, there is firm evidence that microvascular density in PDAC is comparable to that of other adenocarcinomas; moreover, VEGF expression levels are a significant and independent prognostic factor for advanced PDAC,[28] and overexpression of asTF does increase *VEGFA* expression in PDAC cells (Fig. 4*f*). In this light, the increase in vascular density in our mouse model might be due to asTF-mediated induction of *EFEMP1*, which has been recently shown to activate *VEGF* and, subsequently, increase microvascular density in a PDAC model[22]: Thus, we plan to assess the significance of the *EFEMP1* expression for the asTF-PDAC axis with and without EGFR signaling inhibitors in future studies.

Pancreatic cancer is associated with increased thrombosis, and VTE is a risk factor of mortality in most forms of cancers.[29] Haas *et al*. previously demonstrated that pancreas TF is substantially more immunoreactive in pancreatic cancer patients compared to those with chronic pancreatitis; importantly, plasma TF levels were heightened in patients with pancreatic cancer *vs*. controls and were particularly appreciable in patients that developed upper jugular and splenic vein thrombosis.[12] A recent study by Wang *et al*. revealed that the major source of TF activity affording systemic activation of coagulation in PDAC in the tumor itself, whereby clotting factors enter the tumor through neovessels and activate coagulation in a TF-dependent manner.[30] Our study shows that asTF may possibly synergize with flTF in promoting thrombosis in PDAC. We show that asTF overexpressing PDAC cells are more procoagulant and that MPs derived from these cells also display an enhanced TF procoagulant activity. Overexpression of asTF resulted in an enhanced cell surface membrane retention of asTF, but no significant change was observed in flTF levels. The increased asTF retention on the cell membrane is perhaps due to its interaction with integrins which is not likely to affect asTF's ability to bind FVIIa. Indeed, flTF in complex with β1 integrin on MPs appears to have full coagulant function, suggesting that the FVII binding site is preserved in integrin-bound TF.[31] As asTF contains the FVIIa binding domain of flTF, it is possible that asTF binding to FVIIa leads to the overall augmentation of FX-to-FXa conversion in the presence of flTF on cell surfaces. We note that asTF retention may also be accomplished through direct interaction with phospholipid bilayers.[6] As to the ability of asTF to increase flTF levels on PDAC cell-derived MPs, our findings closely echo those recently reported by Garnier *et al*., whereby promotion of EMT in colorectal cancer cells led to the release of extracellular vesicles carrying TF coagulant activity[32]; addition of

asTF to MPs derived from Pt45P1 cells did not augment total TF activity (Fig. 5*f*), suggesting that the procoagulant potential of PDAC cell-derived MPs, while indirectly modulated by asTF, may very well be largely flTF-dependent. Further studies are required to evaluate the kinetics and avidity of asTF.FVIIa interaction and the evidently EMT-mediated mechanisms underlying the enhanced presence of flTF on MPs derived from PDAC cells overexpressing asTF. In sum, our results point to the role of asTF in the pathobiology of PDAC. The minimally coagulant asTF—a molecule that is not likely to significantly contribute to normal hemostasis yet may play a role in cancer-associated thrombosis as well as tumor spread—may serve as a novel target to treat PDAC and its thrombotic complications.

Supplementary Material

Refer to Web version on PubMed Central for supplementary material.

Acknowledgments

Grant sponsor: NIH/NCI; **Grant number:** 1R21CA160293-01A1

The authors thank Vallabaprabhu Subramanya for help with FACS analysis, Birgit Ehmer for help with microscopy, Katie LaSance and Evgeny Ozhegov for help with *in vivo* imaging studies, Neil Batra for help with intracardiac puncture procedure and Ryan Keil for help with tissue culture maintenance.

References

1. Jemal A, Siegel R, Ward E, et al. Cancer statistics, 2008. CA Cancer J Clin. 2008; 58:71–96. [PubMed: 18287387]
2. Rak J, Yu JL, Luyendyk J, et al. Oncogenes, Trousseau syndrome, and cancer-related changes in the coagulome of mice and humans. Cancer Res. 2006; 66:10643–6. [PubMed: 17108099]
3. Tesselaar ME, Romijn FP, van der Linden IK, et al. Microparticle-associated tissue factor activity: a link between cancer and thrombosis? J Thromb Haemost. 2007; 5:520–7. [PubMed: 17166244]
4. Zwicker JI, Liebman HA, Neuberg D, et al. Tumor-derived tissue factor-bearing microparticles are associated with venous thromboembolic events in malignancy. Clin Cancer Res. 2009; 15:6830–40. [PubMed: 19861441]
5. Thomas GM, Panicot-Dubois L, Lacroix R, et al. Cancer cell-derived microparticles bearing P-selectin glycoprotein ligand 1 accelerate thrombus formation in vivo. J Exp Med. 2009; 206:1913–27. [PubMed: 19667060]
6. Bogdanov VY, Balasubramanian V, Hathcock J, et al. Alternatively spliced human tissue factor: a circulating, soluble, thrombogenic protein. Nat Med. 2003; 9:458–62. [PubMed: 12652293]
7. van den Berg YW, van den Hengel LG, Myers HR, et al. Alternatively spliced tissue factor induces angiogenesis through integrin ligation. Proc Natl Acad Sci USA. 2009; 106:19497–502. [PubMed: 19875693]
8. Srinivasan R, Ozhegov E, van den Berg YW, et al. Splice variants of tissue factor promote monocyte-endothelial interactions by triggering the expression of cell adhesion molecules via integrin-mediated signaling. J Thromb Haemost. 2011; 9:2087–96. [PubMed: 21812913]
9. Sawai H, Okada Y, Funahashi H, et al. Interleukin-1alpha enhances the aggressive behavior of pancreatic cancer cells by regulating the alpha6beta1-integrin and urokinase plasminogen activator receptor expression. BMC Cell Biol. 2006; 20:7–8.
10. Goldin-Lang P, Tran QV, Fichtner I, et al. Tissue factor expression pattern in human non-small cell lung cancer tissues indicate increased blood thrombogenicity and tumor metastasis. Oncol Rep. 2008; 20:123–8. [PubMed: 18575726]

11. Rollin J, Regina S, Gruel Y. Tumor expression of alternatively spliced tissue factor is a prognostic marker in non-small cell lung cancer. J Thromb Haemost. 2010; 8:607–10. [PubMed: 19995406]
12. Haas SL, Jesnowski R, Steiner M, et al. Expression of tissue factor in pancreatic adenocarcinoma is associated with activation of coagulation. World J Gastroenterol. 2006; 12:4843–9. [PubMed: 16937466]
13. Hobbs JE, Zakarija A, Cundiff DL, et al. Alternatively spliced human tissue factor promotes tumor growth and angiogenesis in a pancreatic cancer tumor model. Thromb Res. 2007; 120:S13–S21. [PubMed: 18023707]
14. Khorana AA, Ahrendt SA, Ryan CK, et al. Tissue factor expression, angiogenesis, and thrombosis in pancreatic cancer. Clin Cancer Res. 2007; 13:2870–5. [PubMed: 17504985]
15. Tardos JG, Eisenreich A, Deikus G, et al. SR proteins ASF/SF2 and SRp55 participate in tissue factor biosynthesis in human monocytic cells. J Thromb Haemost. 2008; 6:877–84. [PubMed: 18315555]
16. Kirchhofer D, Moran P, Chiang N, et al. Epitope location on tissue factor determines the anticoagulant potency of monoclonal anti-tissue factor antibodies. Thromb Haemost. 2000; 84:1072–81. [PubMed: 11154116]
17. Sipos B, Möser S, Kalthoff H, et al. A comprehensive characterization of pancreatic ductal carcinoma cell lines: towards the establishment of an in vitro research platform. Virchows Arch. 2003; 442:444–52. [PubMed: 12692724]
18. Qi X, Chu Z, Mahller YY, Stringer KF, et al. Cancer-selective targeting and cytotoxicity by liposomal-coupled lysosomal saposin C protein. Clin Cancer Res. 2009; 15:5840–51. [PubMed: 19737950]
19. Olive KP, Jacobetz MA, Davidson CJ, et al. Inhibition of hedgehog signaling enhances delivery of chemotherapy in a mouse model of pancreatic cancer. Science. 2009; 324:1457–61. [PubMed: 19460966]
20. Morello V, Cabodi S, Sigismund S, et al. β1 integrin controls EGFR signaling and tumorigenic properties of lung cancer cells. Oncogene. 2011; 30:4087–96. [PubMed: 21478906]
21. Balanis N, Yoshigi M, Wendt MK, et al. β3 integrin-EGF receptor cross-talk activates p190RhoGAP in mouse mammary gland epithelial cells. Mol Biol Cell. 2011; 22:4288–301. [PubMed: 21937717]
22. Seeliger H, Camaj P, Ischenko I, et al. EFEMP1 expression promotes in vivo tumor growth in human pancreatic adenocarcinoma. Mol Cancer Res. 2009; 7:189–98. [PubMed: 19208748]
23. Yotsumoto F, Fukami T, Yagi H, et al. Amphiregulin regulates the activation of ERK and Akt through epidermal growth factor receptor and HER3 signals involved in the progression of pancreatic cancer. Cancer Sci. 2010; 101:2351–60. [PubMed: 20726858]
24. Schoppmann SF, Birner P, Stöckl J, et al. Tumor-associated macrophages express lymphatic endothelial growth factors and are related to peritu-moral lymphangiogenesis. Am J Pathol. 2002; 161:947–56. [PubMed: 12213723]
25. Yu JL, May L, Lhotak V, et al. Oncogenic events regulate tissue factor expression in colorectal cancer cells: implications for tumor progression and angiogenesis. Blood. 2005; 105:1734–41. [PubMed: 15494427]
26. van den Berg YW, Osanto S, Reitsma PH, et al. The relationship between tissue factor and cancer progression: insights from bench and bedside. Blood. 2012; 119:924–32. [PubMed: 22065595]
27. Camaj P, Seeliger H, Ischenko I, et al. EFEMP1 binds the EGF receptor and activates MAPK and Akt pathways in pancreatic carcinoma cells. Biol Chem. 2009; 390:1293–302. [PubMed: 19804359]
28. Mizukami Y. Bone marrow-derived proangiogenic cells in pancreatic cancer. J Gastroenterol Hepatol. 2012; 27(Suppl 2):23–6. [PubMed: 22320912]
29. Thaler J, Ay C, Mackman N, et al. Microparticle-associated tissue factor activity, venous thromboembolism and mortality in pancreatic, gastric, colorectal and brain cancer patients. J Thromb Haemost. 2012; 10:1363–70. [PubMed: 22520016]
30. Wang JG, Geddings JE, Aleman MM, et al. Tumor-derived tissue factor activates coagulation and enhances thrombosis in a mouse xenograft model of human pancreatic cancer. Blood. 2012; 119:5543–52. [PubMed: 22547577]

31. Ettelaie C, Collier ME, Mei MP, et al. Enhanced binding of tissue factor-microparticles to collagen-IV and fibronectin leads to increased tissue factor activity in vitro. Thromb Haemost. 2013; 109:61–71. [PubMed: 23152142]

32. Garnier D, Magnus N, Lee TH, et al. Cancer cells induced to express mesenchymal phenotype release exosome-like extracellular vesicles carrying tissue factor. J Biol Chem. 2012; 287:43565–72. [PubMed: 23118232]

What's new?

Alternatively spliced tissue factor (asTF) triggers the growth of new blood vessels and is present at elevated levels in certain cancers, indicating that it could play an important role in tumor growth and metastasis. Here, asTF was found to be abundant in human pancreatic ductal adenocarcinoma (PDAC) lesions and stromal monocytes, and its overexpression potentiated PDAC metastasis in vivo. Furthermore, asTF augmented EGFR-linked signaling pathways in PDAC cells and contributed to the coagulant activity of PDAC cells and cell-derived microparticles. The findings suggest that asTF may be a key target for stemming metastatic spread and complications in PDAC.

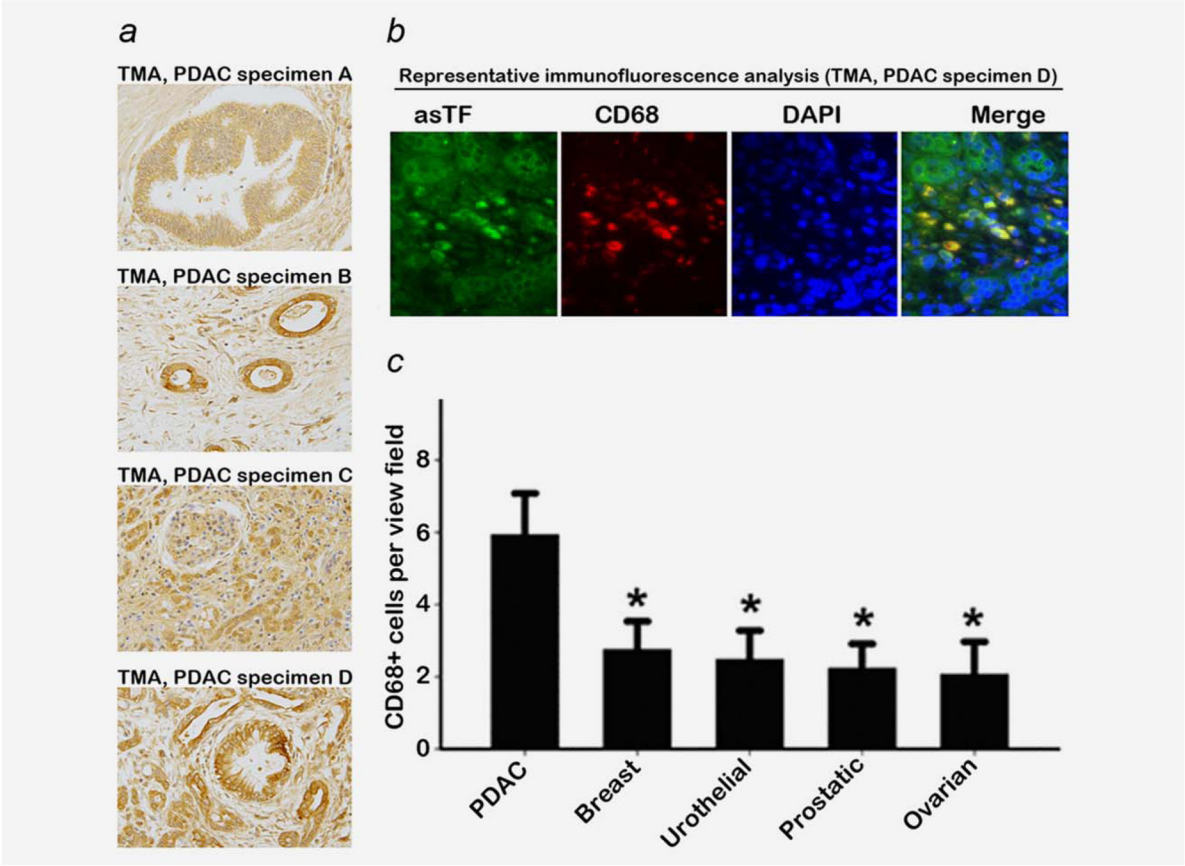

Figure 1.

asTF expression in human adenocarcinoma lesions (original magnification: ×40). *(a)* asTF expression in TMA: specimen A—a diffuse staining pattern of asTF in PanIN; specimen B—cell surface expression of asTF; specimens C and D—asTF expression in highly aggressive PDAC. *(b)* CD68 staining of specimen D (original magnification: ×10X, primary antibody was used at 2.0 μg/mL); asTF expression is observed in the lesion, stroma and infiltrating monocytes. *(c)* Monocyte infiltration in various solid tumors; $*p < 0.05$. [Color figure can be viewed in the online issue, which is available at wileyonlinelibrary.com.]

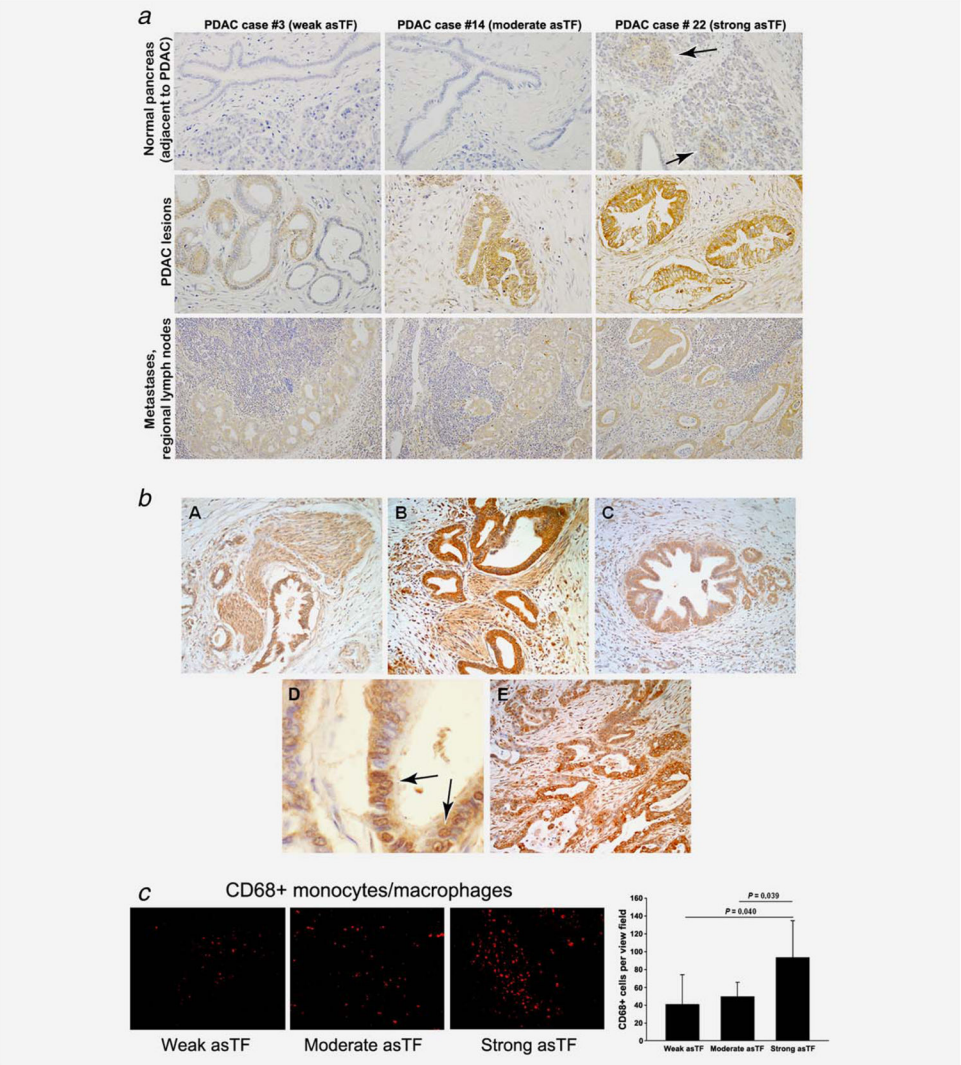

Figure 2.

asTF expression in human PDAC lesions. *(a)* Representative images, top row: staining for asTF in non-malignant pancreas, *i.e*., duct cells, islets of Langerhans (indicated by arrows) and acinar tissue; middle row, staining for asTF in PDAC lesions (weak staining, ~15%; moderate staining, ~70%; strong staining, ~15% of all tissue specimens, $n = 29$); bottom row, PDAC metastases in regional lymph nodes. Custom anti-asTF polyclonal antibody was used at 2.0 μg/mL; original magnification: ×40. *(b)* Expression patterns of asTF in PDAC. Representative histological sections showing asTF staining patterns in PDAC displaying perineural invasion (images A and B), pancreatic intraepithelial neoplasia lesions (image C) and (peri)nuclear staining occasionally observed in PDAC cells, arrows (image D). Intra-lesional variability of asTF protein expression was also observed in some PDAC specimens (image E). *(c)* CD68 staining in PDAC specimens exhibiting weak, moderate and strong staining for asTF (original magnification: ×40, staining was carried out as in Fig. 1). [Color figure can be viewed in the online issue, which is available at wileyonlinelibrary.com.]

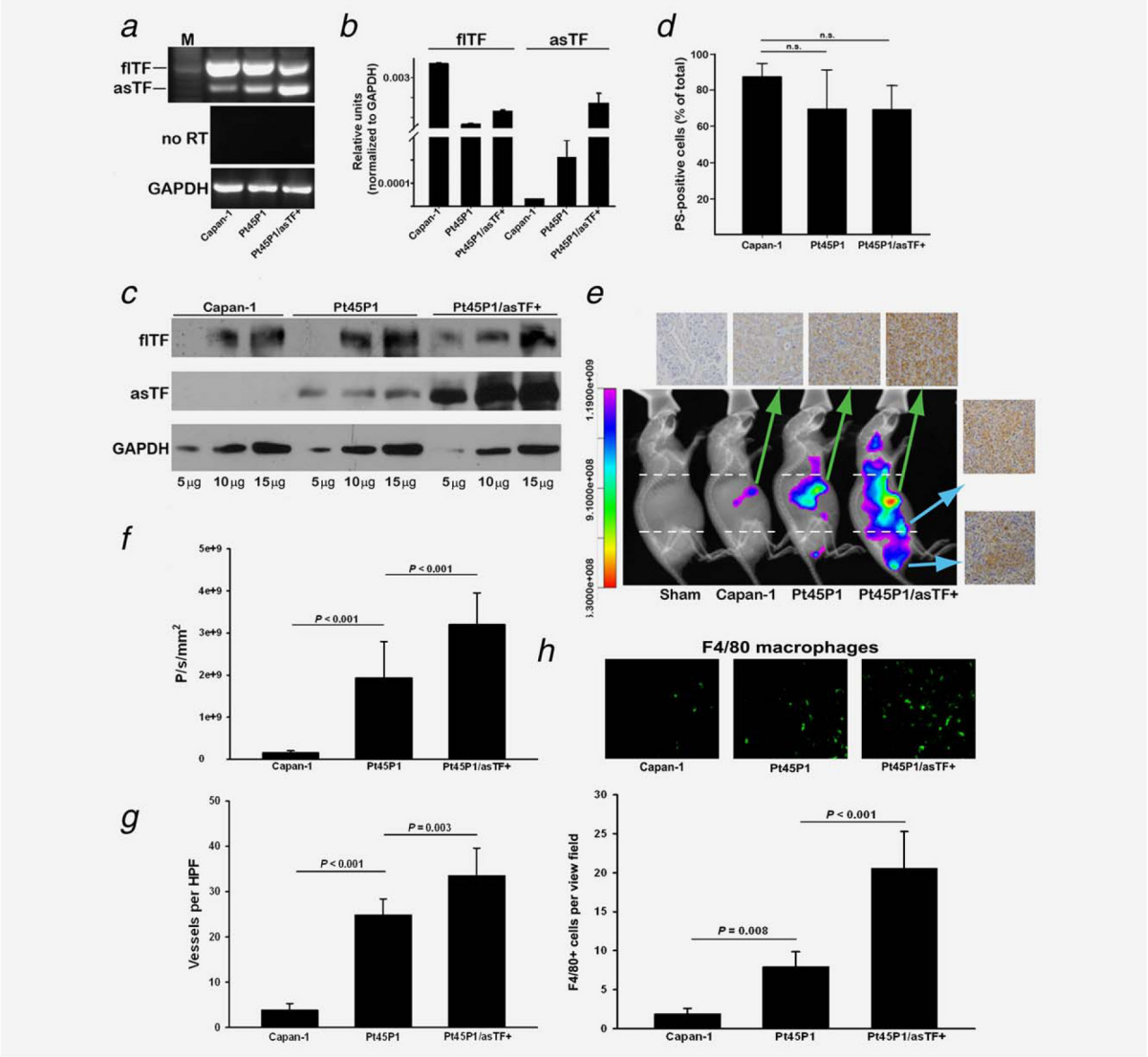

Figure 3.

asTF promotes PDAC spread *in vivo*. *(a,b)* Assessment of the three PDAC lines for flTF/asTF expression by conventional and quantitative real-time RT-PCR as described[15] ($n = 3$). *(c)* flTF/asTF protein levels in cell lysates (total protein, μg). *(d)* Annexin-V staining of the PDAC cell lines by flow cytometry ($n = 3$). *(e)* PDAC cell lines were implanted orthotopically (three independent experiments, three mice per cohort), and 3.5 weeks post-surgery the animals were imaged *in vivo* using CVM-SapC(H2)-DOPS *via* tail vein injection. The mice were then sacrificed, tumors were excised, formalin fixed/paraffin embedded and stained for asTF (top row); side panel—isolated Pt45P1/asTF+ lymph node metastases. *(f)* Quantification of tumor spread to distal lymph nodes (analyzed areas were above and below the dashed lines shown in Fig. 3*e*). (*g*) Vessel density assessment by isolectin B4 staining of the excised tumors. (*h*) Infiltration of tumor stroma assessed by anti-

F4/80 staining; representative images are shown on top; eight view fields per specimen (n = 3 per specimen type) were counted and averaged; primary antibody was used at 10.0 μg/mL. [Color figure can be viewed in the online issue, which is available at wileyonlinelibrary.com.]

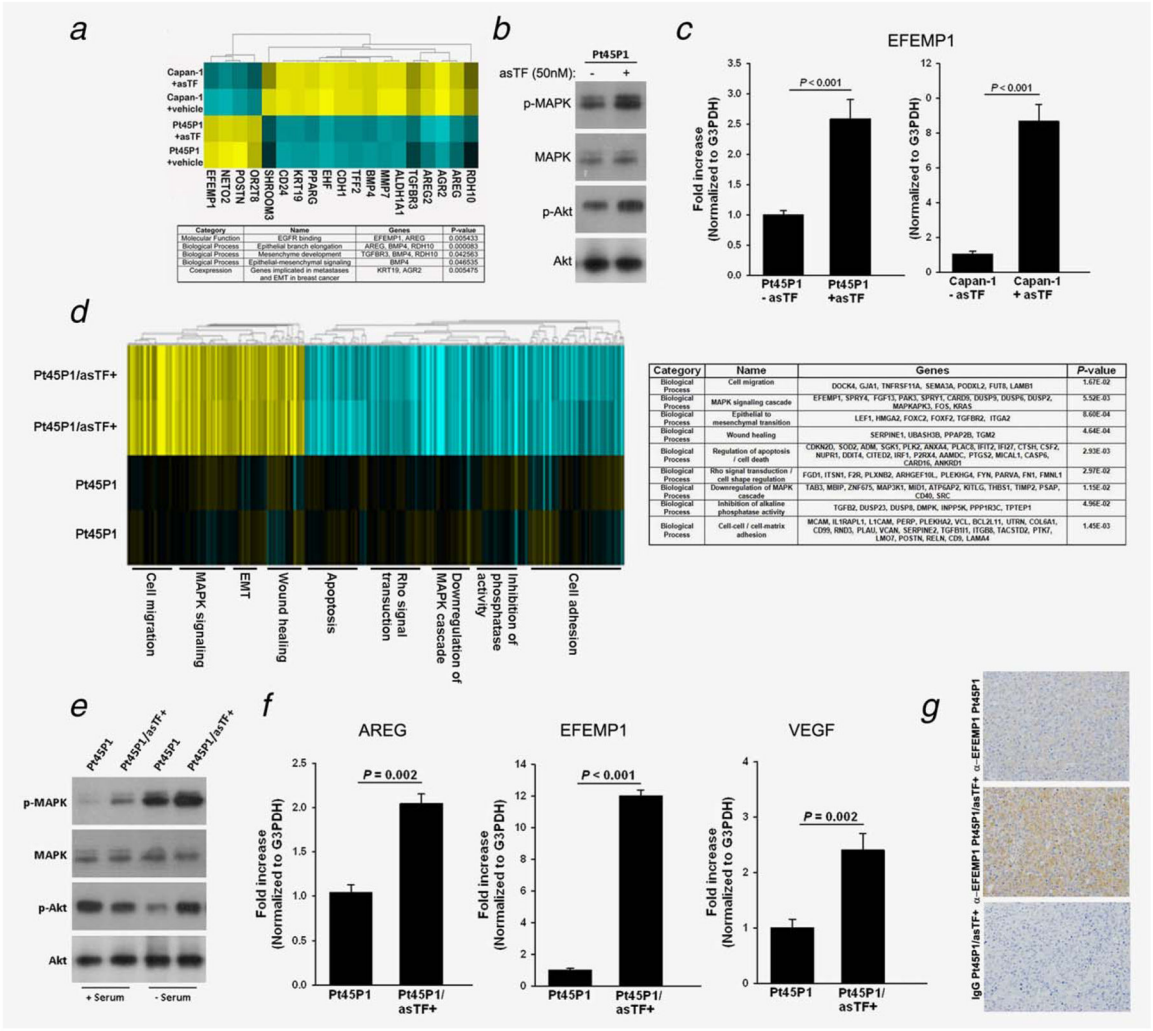

Figure 4.

asTF protein elicits changes in gene expression in PDAC cells (representative data, two independent experiments performed in duplicate). *(a)* Heat map, Capan-1 and Pt45P1 cells were treated with recombinant asTF (50 nM) or vehicle control (PBS/glycerol) for 4 hours, total RNA was reverse transcribed, amplified, fragmented and labeled for microarray analysis; table: summary of the biological processes significantly altered in PDAC cells Capan-1 and Pt45P1. (*b*) Western blotting, phosphorylation status of MAPK and Akt in Pt45P1 cells treated with recombinant asTF or vehicle control; real-time quantitative RT-PCR, levels of *EFEMP1* transcripts in Capan-1 and Pt45P1 cells treated with recombinant asTF or vehicle control. (*d*) Heat map, differences in gene expression between Pt45P1 and Pt45P1/asTF+ cells; table: summary of the biological processes significantly altered in Pt45P1/asTF+ cells. (*e*) Western blotting, phosphorylation status of MAPK and Akt in Pt45P1 cells and Pt45P1/asTF+ cells. (*f*) Real-time quantitative RT-PCR, levels of *EFEMP1*, *AREG* and *VEGFA* transcripts in Pt45P1 cells and Pt45P1/asTF+ cells. (*g*) Immunohistochemical analysis of EFEMP1 protein expression in Pt45P1 and Pt45P1/asTF+

cells. [Color figure can be viewed in the online issue, which is available at wileyonlinelibrary.com.]

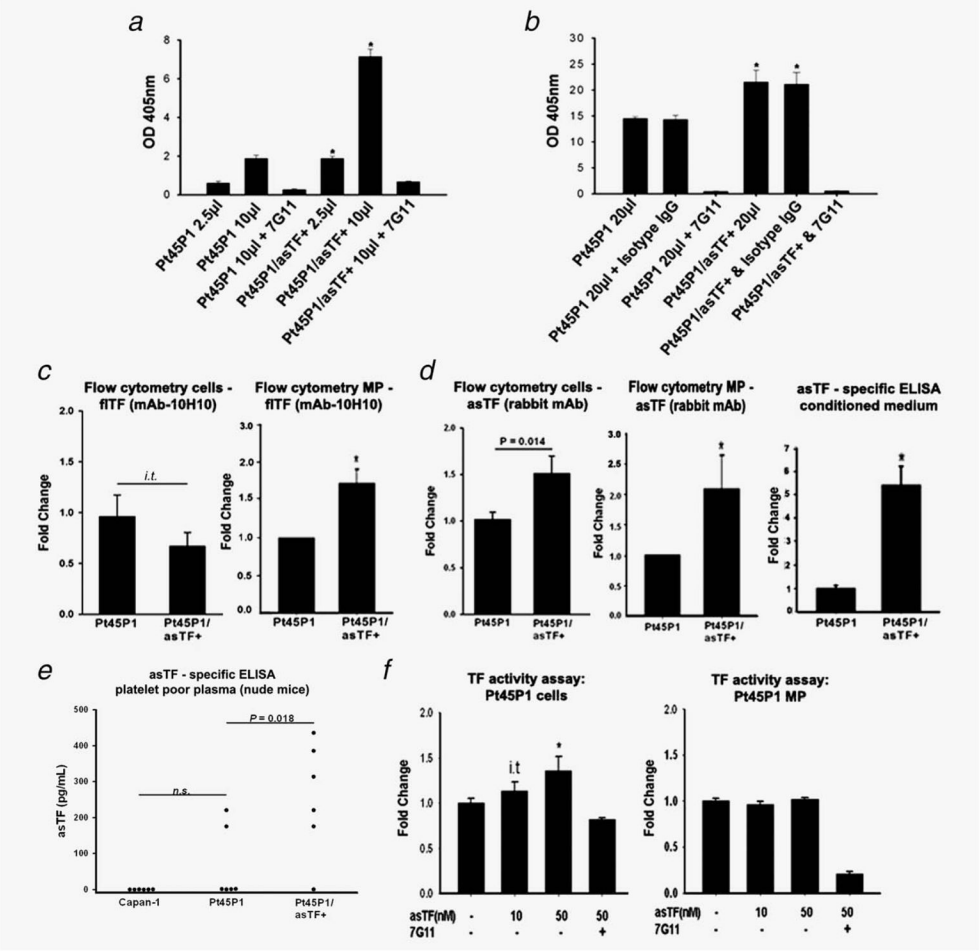

Figure 5.

Analysis of procoagulant activity in PDAC cell lines and determination of TF isoform levels on nonpermeabilized cells and cell-derived MPs ($n \geq 3$ experiments per each sample type). *(a)* TF activity on cell surfaces. *(b)* TF activity on cell-derived MP. *(c)* Cell-surface and MP expression of flTF protein. *(d)* Cell surface and MP expression of asTF protein; levels of asTF secreted in the culture media. *(e)* Levels of asTF protein in the plasma of mice bearing tumors as indicated (six plasma samples per type, collected during two independent *in vivo* studies). *(f)* Effect of recombinant asTF on TF procoagulant activity on the surfaces of intact cells and cell-derived MP. $*p < 0.05$, i.t –in-trend, $0.1 < p < 0.05$.